

Planar Hexacoordinate Carbons: Half Covalent, Half Ionic

Luis Leyva-Parra,^a Luz Diego,^b Osvaldo Yañez,^{a,c} Diego Inostroza,^a Jorge Barroso,^{d,*}

Alejandro Vásquez-Espinal,^{a,*} Gabriel Merino^{d,*} and William Tiznado.^{a,*}

*^aComputational and Theoretical Chemistry Group, Departamento de Ciencias Químicas,
Facultad de Ciencias Exactas, Universidad Andres Bello, República 498, Santiago, Chile*

*^bEscuela Profesional de Química, Facultad de Ciencias Naturales, Universidad Nacional
Federico Villarreal, Jr. Río Chepén 290, El Agustino, Lima, Perú*

^cCenter of New Drugs for Hypertension (CENDHY), Santiago, Chile

*^dDepartamento de Física Aplicada, Centro de Investigación y de Estudios Avanzados, Unidad
Mérida, km. 6 Antigua carretera a Progreso. Apdo. Postal 73, Cordemex, Mérida, Yuc., México*

E-mail: a.vasquezespinal@uandresbello.edu

wtiznado@unab.cl

jorge.barroso@cinvestav.mx

gmerino@cinvestav.mx

Abstract

The global minima of thirteen combinations of atoms with formula CE_3M_3^+ ($\text{E}=\text{S-Te}$ and $\text{M}=\text{Li-Cs}$) adopt a planar structure with carbon covalently bonded to three chalcogens and ionically bonded to the three alkali-metals to stabilize the first global minima structures containing planar hexacoordinate carbon atoms.

In 1970, Hoffmann and co-workers stated that incorporating π -acceptor/ σ -donor ligands could stabilize a transition state with a planar tetracoordinate carbon (ptC).¹ The approach was successfully adopted by the group of Schleyer to stabilize a local minimum with this peculiar form.² The first experimental example of a ptC took place inadvertently in 1977,³ paving the way for synthesizing new ptCs. This led to extensive experimental and theoretical efforts to search for anti-van't Hoff/Le Bel molecules.⁴⁻⁸ These findings inspired the design of more ptCs, and later extended to highly coordinated species.⁹⁻¹⁵ However, as the coordination number increases, the more elusive these species become. So far, only a handful of global minima structures with a planar pentacoordinate carbon (ppC) are known,^{10,16} and not a single planar hexacoordinate carbon (phC). Note that the reported Be_2C monolayer is a global minimum with a quasi-planar hexacoordinate carbon moiety.¹⁷

The D_{6h} CB_6^{2-} cluster (**1**) was the first phC candidate,¹⁸ but it is $34.4 \text{ kcal}\cdot\text{mol}^{-1}$ higher in energy than its most stable isomer.¹⁹ Although **1** is only a local minimum, this cluster was used as a framework by Wu et al.²⁰ to design, via isoelectronic substitution, two additional phC candidates with D_{3h} symmetry, Be_3CN_3^+ and Li_3CO_3^+ (**2** and **3** in Figure 1). The authors located **2** at $6.1 \text{ kcal}\cdot\text{mol}^{-1}$ above the lowest-lying energy isomer and **3** as the putative global minimum.

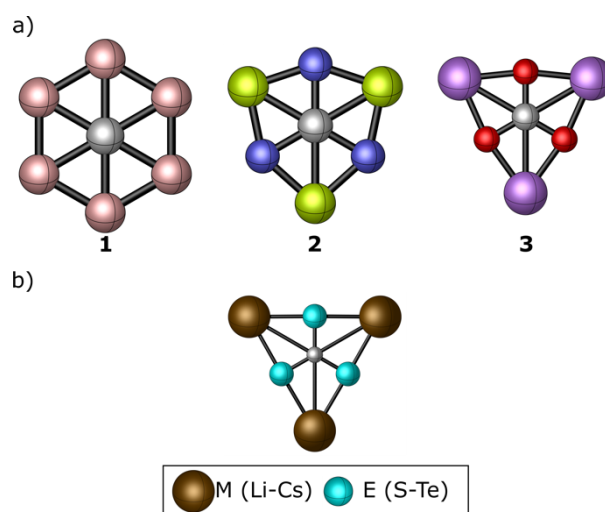
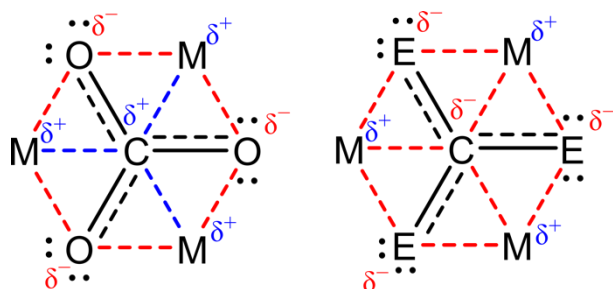


Figure 1. a) CB_6^{2-} (**1**), CN_3Be_3^+ (**2**), and Li_3CO_3^+ (**3**) derivatives and b) their corresponding CE_3M_3^+ analogues.

According to the authors, the carbonate dianion CO_3^{2-} is electrostatically stabilized by the three bridging Li^+ counterions in **3**. Since the C–Li contacts are shorter than the C–Li distances in the methyllithium tetramer and hexamer (2.31 Å),²¹ carbon “touches” the six atoms around, i.e., based on a geometrical criterion, the hexacoordination was assumed. IUPAC defines the coordination number of a specified atom in a chemical species as “the number of other atoms directly linked to that specified atom”.²² So, the question remaining is whether the C is truly hexacoordinate. Our computations indicate positive natural charges on C and Li atoms in **3** ($q_c = +0.87 |e|$ and $q_{\text{Li}} = +0.97 |e|$), implying electrostatic repulsion between them. The interacting quantum atoms (IQA) analysis supports a strong repulsion between carbon and lithium (324.2 kcal.mol⁻¹), mostly pure coulombic repulsion (324.6 kcal.mol⁻¹, see Table S1 in the ESI). Indeed, the positive charge on C is expected due to the electronegativity difference between C and O ($\Delta\chi = 1.0$) (Scheme 1, left). How to induce the electrostatic interaction between carbon and the alkali metals? Our idea is to replace oxygen with

heavier (and less electronegative) chalcogens in **3**, stabilizing a true planar hexacoordinate carbon atom (Scheme 1, right). From the fifteen possible CE_3M_3^+ ($\text{E} = \text{S-Te}$ and $\text{M} = \text{Li-Cs}$) combinations, thirteen of them satisfy all conditions to be classified as phC.



Scheme 1. Schematic hybrid structures of the CO_3^{2-} (left) and hypothetical CE_3^{2-} (right) moieties stabilized by Li^+ and alkali cations (M^+), respectively. Red and blue dotted lines represent attractive and repulsive electrostatic interactions, respectively.

A systematic exploration of the potential energy surfaces was carried out using the AUTOMATON²³ and GLOMOS²⁴ programs. The initial screening in the singlet and triplet states was done at the PBE0²⁵-D3²⁶/SDDALL^{27,28} level. The low-lying energy isomers ($< 30 \text{ kcal.mol}^{-1}$ above the putative global minimum) were reminimized at the PBE0-D3/def2-TZVP²⁹ level, and relative energies were computed at the CCSD(T)^{30,31}/def2-TZVP//PBE0-D3/def2-TZVP level. So, for the energetic discussion, only the latter level is considered. The diagnostic of the T_1 coupled-cluster operator was performed to verify whether the converged CCSD wave functions are based on a single-reference method.³² All the T_1 values are lower than the suggested threshold of 0.02 (Table S1). These computations were done using Gaussian 16.³³

The bonding was analyzed in terms of the Wiberg bond index (WBI)³⁴ and natural population analysis (NPA),³⁵ as implemented in the NBO 6.0 program.³⁶ Additionally,

the Adaptive Natural Density Partitioning (AdNDP) method was used.^{37,38} AdNDP recovers the electron pair Lewis concept as the fundamental component of chemical bonding, localizing the n-center-two-electron bonds (nc-2e). Additionally, IQA³⁹ was used to decompose the interaction energy. IQA rises from a competition between atomic deformation and the additive interatomic interaction energies. The former is an analogue of the classical promotion energy necessary for one atom to bond to another. The latter is composed of classical (or ionic-type) and exchange-correlation (or covalent-type) components. So, the interatomic interaction energy, V_{int} , is the sum of the coulombic, V_{C} , and exchange-correlation, V_{XC} , terms, where V_{C} is the exact electrostatic interaction between the electrons and nuclei contained in a pair of basins and includes all the classical electrostatic terms (nuclear repulsion, electron-nucleus attraction, and the Coulomb part of the electron-electron repulsion). The term V_{XC} is purely quantum mechanical in nature, depending only on the exchange-correlation part of the electron-electron interaction. Usually, while V_{C} is related to the ionic-type component of a given interaction, and V_{XC} to electron-sharing or covalent-type interaction.

All the global minima of the CE_3M_3^+ ($\text{E} = \text{O-Te}$ and $\text{M} = \text{Li-Cs}$) clusters adopt a planar D_{3h} symmetry with C-E distances between a single and a double bond (see Table 1). This is consistent with the corresponding WBI values (1.25 - 1.34), which is an estimation of the bond order from the natural population analysis. Table 1 shows that the C-M distances are longer than the expected single bond⁴⁰ but shorter than the sum of their van der Waals radii. So, it could be considered that in these clusters, carbon “touches” the six surrounding atoms, that is, based on geometrical criteria, all of them contain a phC, as suggested by Wu et al.¹⁵

Remarkably, except for $\text{CSe}_3\text{Li}_3^+$ and $\text{CTe}_3\text{Li}_3^+$, the remaining planar D_{3h} stoichiometries are the putative global minima (see Figures S1-S13 and the

corresponding Cartesian coordinates in the supplementary information). In all cases, the smallest vibrational frequencies are reasonably large (10 - 178 cm^{-1}), the singlet state is the most favorable one (the energy difference with the closest triplet ranges from 19.0 to 118.1 kcal.mol^{-1}) and the HOMO-LUMO energy gaps are relatively high, varying between 3.15 and 8.34 eV (Table 1).

NPA charges support that the CE_3 moiety is a dianion electrostatically stabilized by three M^+ ions. Besides, the low WBI values (0.02 - 0.10) of the peripheral E-M might indicate ionic bonding, which is relevant because ligand-ligand interactions contribute significantly to the stabilization of planar hypercoordinate species. Note that the lowest E-M WBIs occur in systems with oxygen. However, the C-M WBI values are zero, and it is not clear if there is an ionic interaction or any interaction at all between the center and the alkali-metals. Although in the clusters with heavier chalcogens, contrary to CO_3M_3^+ systems, the charge on the carbon atom is negative, suggesting a probable electrostatic interaction with the alkali-metal cation. The negative charge on C increases as the electronegativity of the chalcogen decreases ($q(\text{C})$ is approximately -0.5, -0.7, and -1.0 $|e|$ for S, Se, and Te, respectively), while the charge on the alkali-metal cations has no significant variation. So, the zero C-M WBI values might be the consequence of a pure electrostatic interaction without any orbital overlap involved.

Table 1. Distances (r , Å), charges (q , $|e|$), Wiberg bond indices (WBI), HOMO-LUMO gap ($\Delta E_{\text{H-L}}$, eV), and the lowest harmonic vibrational frequency (ν_{min} , cm^{-1}) of the CE_3M_3^+ ($\text{E}=\text{O-Te}$ and $\text{M}=\text{Li-Cs}$) computed at the PBE0-D3/def2-TZVP level.

System	$r_{\text{C-Ch}}$	$r_{\text{C-M}}$	$r_{\text{Ch-M}}$	$q(\text{C})$	$q(\text{E})$	$q(\text{M})$	$\text{WBI}_{\text{C-E}}$	$\text{WBI}_{\text{E-M}}$	$\Delta E_{\text{H-L}}$	ν_{min}
CO_3Li_3	1.28	2.18	1.90	0.87	-0.92	0.97	1.29	0.02	8.34	178
CO_3Na_3	1.29	2.55	2.21	0.90	-0.94	0.97	1.29	0.02	6.21	103

CO₃K₃	1.29	2.92	2.54	0.91	-0.94	0.97	1.28	0.02	5.51	75
CO₃Rb₃	1.29	3.10	2.69	0.91	-0.95	0.98	1.28	0.02	5.05	63
CO₃Cs₃	1.29	3.22	2.81	0.92	-0.94	0.97	1.28	0.03	5.32	50
CS₃Li₃	1.71	2.67	2.34	-0.52	-0.41	0.92	1.34	0.07	5.06	54
CS₃Na₃	1.72	3.08	2.68	-0.51	-0.42	0.93	1.34	0.06	4.72	47
CS₃K₃	1.72	3.51	3.04	-0.49	-0.45	0.95	1.33	0.04	4.48	37
CS₃Rb₃	1.72	3.70	3.21	-0.49	-0.45	0.95	1.33	0.04	4.37	30
CS₃Cs₃	1.72	3.84	3.34	-0.49	-0.45	0.95	1.33	0.04	4.37	26
CSe₃Na₃	1.86	3.23	2.81	-0.70	-0.35	0.91	1.31	0.07	4.19	32
CSe₃K₃	1.86	3.67	3.18	-0.68	-0.38	0.94	1.31	0.05	3.97	24
CSe₃Rb₃	1.86	3.87	3.36	-0.68	-0.38	0.95	1.31	0.05	3.87	19
CSe₃Cs₃	1.86	4.03	3.49	-0.68	-0.39	0.95	1.31	0.05	3.86	14
CTe₃Na₃	2.07	3.47	3.02	-1.02	-0.21	0.89	1.25	0.10	3.43	22
CTe₃K₃	2.07	3.92	3.40	-1.01	-0.26	0.93	1.25	0.06	3.26	18
CTe₃Rb₃	2.07	4.12	3.57	-1.01	-0.26	0.93	1.25	0.06	3.16	14
CTe₃Cs₃	2.07	4.29	3.72	-1.01	-0.26	0.93	1.25	0.06	3.15	11

The sums of Pyykkö's single bond-radii for the C-Li, C-Na, C-K, C-Rb, and C-Cs bonds are 2.08, 2.30, 2.71, 2.85 and 3.07 Å, respectively.⁴⁰ The sums of van der Waals radii for the C-Li, C-Na, C-K, C-Rb, and C-Cs bonds are 3.82, 4.20, 4.43, 4.91 and 5.18 Å, respectively.⁴¹

The charge analysis and bond orders are in line with the picture obtained from AdNDP. Let us analyze CSe₃K₃⁺ as an example. The AdNDP recovers three 2c-2e C-Se σ-bonds and three delocalized π-bonds spread on the CSe₃ moiety, implying, once more, that if there is any interaction between CE₃ and the cations, it would be purely

electrostatic. These bonding patterns were found for the other CE_3M_3^+ systems (see Table S3). A different situation occurs in CB_6^{2-} . Its covalent character is corroborated by the WBI values and the AdNDP analysis (Figure 2). There is a set of six peripheral 2c-2e B-B σ -bonds, with an occupation number (ON) of 1.95 |e|. For this cluster, the C-B and B-B bond lengths (1.59 Å) are shorter than the corresponding single bond according to the covalent radius of Pyykkö.⁴⁰ Most importantly, there are multicenter bonds between C and B, justifying the carbon hypercoordination. In summary, tools like WBI or AdNDP, designed to understand chemical interactions between atoms with orbital overlap such as C-E, cannot confirm whether the carbon and the alkali-metals are connected. Nonetheless, the charge analysis points to a possible electrostatic interaction between C and M atoms for E = S, Se, and Te.

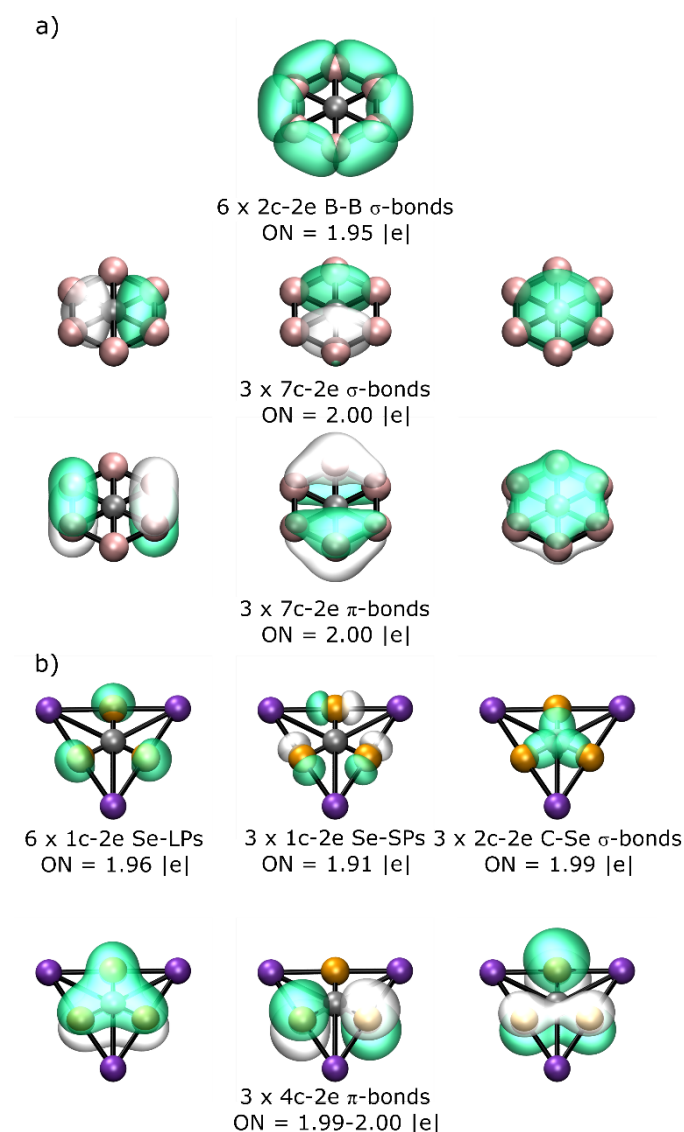


Figure 2. AdNDP analysis of a) CB_6^{2-} and b) CSe_3K_3^+ . ON stands for occupation number.

So, it is mandatory to use a proper methodology to describe ionic interactions. IQA is an option, offering a more accurate description of such types of interactions. Quite recently, this methodology was fundamental to provide clues to explain the chemical bond in NaBH_3^- .⁴² The IQA analysis for the CE_3Na^+ series is shown in Table 2. At first sight, CO_3Na_3^+ is easily distinguishable from the rest. The IQA interaction energy, $V_{\text{IQA}}^{\text{Int}}$, between carbon and oxygen is more than four times greater ($-990.27 \text{ kcal.mol}^{-1}$)

than with any other remaining chalcogen. The same is true for the alkali-metal interaction, which is three to five times larger with oxygen ($-200.74 \text{ kcal.mol}^{-1}$). These strong C-O and O-Na stabilizing interactions occur at the expense of a strong repulsion of the center with the alkali metal ($274.47 \text{ kcal.mol}^{-1}$). This is in perfect agreement with the previous analyses. The higher interaction of carbon and oxygen exceeds the repulsion with sodium, forming a CO_3^{2-} fragment bridged by alkali-metals attracted to the oxygens.

Now, let us analyze the rest of the systems in the series. The IQA interaction energy between the C and each E is the major attractive component. The value decreases in magnitude with heavier chalcogens (from -234.6 to $-215.5 \text{ kcal.mol}^{-1}$). The interactions between peripheral atoms, E-Na, essential for the stabilization of the system, have similar decreasing behavior (from -58.5 to $-38.3 \text{ kcal.mol}^{-1}$). Interestingly, the opposite takes place between carbon and the alkali-metal. The interaction energy increases from S to Te (from -56.0 to $-81.0 \text{ kcal.mol}^{-1}$). But above all, these structures show an electrostatic attraction between the center and sodium, which is essentially coulombic (approximately 99%). This electrostatic interaction between C and M is found in all the global minima of the CE_3M_3^+ (E = S-Te and M = Li-Cs) series (Tables S4-S6). In other words, the systems could be defined as phC , with the central carbon atom covalently bonded to the chalcogens and ionically bonded to the alkali-metals.

Table 2. Energy components of IQA for the D_{3h} CE_3Na_3^+ systems (E=O, S, Se and Te); V_{IQA}^{int} , V_C^{int} , and V_{XC}^{int} are interatomic IQA interaction energy and their coulombic and exchange-correlation energy components, respectively, in kcal.mol⁻¹.

	CO_3Na_3^+	CS_3Na_3^+	$\text{CSe}_3\text{Na}_3^+$	$\text{CTe}_3\text{Na}_3^+$
$V_{IQA}^{Int}(\text{C-E})$	-990.3	-234.6	-215.5	-217.8
$V_C^{Int}(\text{C-E})$	-802.7	-2.9	-9.0	-39.3
$V_{XC}^{Int}(\text{C-E})$	-187.6	-231.6	-206.5	-178.5
$V_{IQA}^{Int}(\text{C-Na})$	274.5	-56.0	-63.1	-81.0
$V_C^{Int}(\text{C-Na})$	274.9	-55.2	-62.4	-80.3
$V_{XC}^{Int}(\text{C-Na})$	-0.4	-0.8	-0.7	-0.6
$V_{IQA}^{Int}(\text{E-Na})$	-200.7	-58.5	-51.0	-38.3
$V_C^{Int}(\text{E-Na})$	-186.6	-45.8	-38.6	-26.3
$V_{XC}^{Int}(\text{E-Na})$	-14.1	-12.6	-12.2	-12.0

In summary, the global minima of thirteen combinations of the CE_3M_3^+ (E = S-Te and M = Li-Cs) series contain a real planar hexacoordinate carbon. The bonding analysis confirms that carbon forms covalent bonds with the chalcogens and ionic bonds with the alkali-metals. These systems contrast with the reported Li_3CO_3^+ because the substitution of oxygen atoms by heavier elements of the same group induces a negative charge in the central carbon, leading to attractive interactions with the alkali-metals. Finally, viable planar hexacoordinate carbon atoms that satisfy all conditions to be classified as phC were found.

The authors are grateful for the financial support of the grants: National Agency for Research and Development (ANID)/Scholarship Program/BECAS DOCTORADO NACIONAL/2019–21190427, National Agency for Research and Development (ANID)/Scholarship Program/BECAS DOCTORADO NACIONAL/2020–21201177 and Fondecyt grant N° 1181165. Powered@NLHPC: This research was partially supported by the supercomputing infrastructure of the NLHPC (ECM-02). The work in Mexico is supported by Grant SEP-Cinvestav-2018-57. J. B. thanks Conacyt for his PhD fellowship.

Conflicts of interest

There are no conflicts to declare.

References

1. Hoffmann, R., Alder, R. W. & Wilcox, C. F. Planar tetracoordinate carbon. *J. Am. Chem. Soc.* **92**, 4992–4993 (1970).
2. Collins, J. B. *et al.* Stabilization of planar tetracoordinate carbon. *J. Am. Chem. Soc.* **98**, 5419–5427 (1976).
3. Cotton, F. A. & Millar, M. The probable existence of a triple bond between two vanadium atoms. *J. Am. Chem. Soc.* **99**, 7886–7891 (1977).
4. Erker, G. Planar-Tetracoordinate Carbon: Making Stable Anti-van' t Hoff/LeBel Compounds. *Comments Inorg. Chem.* **13**, 111–131 (1992).
5. Röttger, D. & Erker, G. Compounds Containing Planar-Tetracoordinate Carbon. *Angew. Chemie Int. Ed. English* **36**, 812–827 (1997).
6. Siebert, W. & Gunale, A. Compounds containing a planar-tetracoordinate carbon atom as analogues of planar methane. *Chem. Soc. Rev.* **28**, 367–371 (1999).
7. Keese, R. Carbon flatland: planar tetracoordinate carbon and fenestranes. *Chem. Rev.* **106**, 4787–4808 (2006).
8. Merino, G., Méndez-Rojas, M. A., Vela, A. & Heine, T. Recent advances in planar tetracoordinate carbon chemistry. *J. Comput. Chem.* **28**, 362–372 (2007).
9. Wang, Z.-X. & Schleyer, P. v. R. Construction principles of "hyparenes": families of molecules with planar pentacoordinate carbons. *Science*, **292**, 2465–2469 (2001).

10. Vassilev-Galindo, V., Pan, S., Donald, K. J. & Merino, G. Planar pentacoordinate carbons. *Nat. Rev. Chem.* **2**, 114 (2018).
11. Grande-Aztatzi, R. *et al.* Planar pentacoordinate carbons in CBe_5^{4-} derivatives. *Phys. Chem. Chem. Phys.* **17**, 4620–4624 (2015).
12. Pei, Y., An, W., Ito, K., Schleyer, P. v. R. & Zeng, X. C. Planar pentacoordinate carbon in CAI_5^+ : a global minimum. *J. Am. Chem. Soc.* **130**, 10394–10400 (2008).
13. Wang, Y., Li, F., Li, Y. & Chen, Z. Semi-metallic Be_3C_2 monolayer global minimum with quasi-planar pentacoordinate carbons and negative Poisson's ratio. *Nat. Commun.* **7**, 11488 (2016).
14. Cui, Z. *et al.* Planar pentacoordinate carbon atoms embedded in a metallocene framework. *Chem. Commun.* **53**, 138–141 (2017).
15. Pan, S. *et al.* Planar pentacoordinate carbon in CGa_5^+ derivatives. *Phys. Chem. Chem. Phys.* **20**, 12350–12355 (2018).
16. Guo, J.-C., Feng, L.-Y., Barroso, J., Merino, G. & Zhai, H.-J. Planar or tetrahedral? A ternary 17-electron CBe_5H_4^+ cluster with planar pentacoordinate carbon. *Chem. Commun.* **56**, 8305–8308 (2020).
17. Li, Y., Liao, Y. & Chen, Z. Be_2C monolayer with quasi-planar hexacoordinate carbons: a global minimum structure. *Angew. Chemie* **126**, 7376–7380 (2014).
18. Exner, K. & Schleyer, P. v. R. Planar hexacoordinate carbon: a viable possibility. *Science* **290**, 1937–1940 (2000).
19. Averkiev, B. B. *et al.* Carbon Avoids Hypercoordination in CB_6^- , CB_6^{2-} , and C_2B_5^- Planar Carbon–Boron Clusters. *J. Am. Chem. Soc.* **130**, 9248–9250 (2008).
20. Wu, Y.-B. *et al.* D_{3h} CN_3Be_3^+ and CO_3Li_3^+ : viable planar hexacoordinate carbon prototypes. *Phys. Chem. Chem. Phys.* **14**, 14760–14763 (2012).
21. Setzer, W. N. & Schleyer, P. v. R. X-ray structural analyses of organolithium compounds. in *Advances in organometallic chemistry* vol. 24 353–451 (Elsevier, 1985).
22. Muller, P. Glossary of terms used in physical organic chemistry (IUPAC Recommendations 1994). *Pure Appl. Chem.* **66**, 1077–1184 (1994).
23. Yañez, O. *et al.* AUTOMATON: a program that combines a probabilistic cellular automata and a genetic algorithm for global minimum search of clusters and molecules. *J. Chem. Theory Comput.* **15**, 1463–1475 (2019).
24. Grande-Aztatzi, R. *et al.* Structural evolution of small gold clusters doped by one and two boron atoms. *J. Comput. Chem.* **35**, 2288–2296 (2014).
25. Adamo, C. & Barone, V. Toward reliable density functional methods without adjustable parameters: The PBE0 model. *J. Chem. Phys.* **110**, 6158–6170 (1999).
26. Grimme, S., Antony, J., Ehrlich, S. & Krieg, H. A consistent and accurate ab initio parametrization of

- density functional dispersion correction (DFT-D) for the 94 elements H-Pu. *J. Chem. Phys.* **132**, 154104 (2010).
27. Fuentealba, P., Von Szentpaly, L., Preuss, H. & Stoll, H. Pseudopotential calculations for alkaline-earth atoms. *J. Phys. B At. Mol. Phys.* **18**, 1287 (1985).
 28. Bergner, A., Dolg, M., Küchle, W., Stoll, H. & Preuss, H. Ab initio energy-adjusted pseudopotentials for elements of groups 13–17. *Mol. Phys.* **80**, 1431–1441 (1993).
 29. Weigend, F. & Ahlrichs, R. Balanced basis sets of split valence, triple zeta valence and quadruple zeta valence quality for H to Rn: design and assessment of accuracy. *Phys. Chem. Chem. Phys.* **7**, 3297–3305 (2005).
 30. Bartlett, R. J. & Musiał, M. Coupled-cluster theory in quantum chemistry. *Rev. Mod. Phys.* **79**, 291 (2007).
 31. Raghavachari, K., Trucks, G. W., Pople, J. A. & Head-Gordon, M. A fifth-order perturbation comparison of electron correlation theories. *Chem. Phys. Lett.* **157**, 479–483 (1989).
 32. Lee, T. J. & Taylor, P. R. A diagnostic for determining the quality of single-reference electron correlation methods. *Int. J. Quantum Chem.* **36**, 199–207 (1989).
 33. Frisch, M. J. *et al.* Gaussian, Inc., Wallingford CT. *Gaussian 16, Revis. B.01* (2016).
 34. Wiberg, K. B. Application of the pople-santry-segal CNDO method to the cyclopropylcarbanyl and cyclobutyl cation and to bicyclobutane. *Tetrahedron* **24**, 1083–1096 (1968).
 35. Reed, A. E., Weinstock, R. B. & Weinhold, F. Natural population analysis. *J. Chem. Phys.* **83**, 735–746 (1985).
 36. Glendening, E. D. *et al.* Natural bond orbital analysis program: NBO 6.0. *Theor. Chem. Institute, Univ. Wisconsin, Madison, WI* (2013).
 37. Zubarev, D. Y. & Boldyrev, A. I. ” Developing paradigms of chemical bonding: adaptive natural density partitioning. *Phys. Chem. Chem. Phys.* **10**, 5207–5217 (2008).
 38. Zubarev, D. Y. & Boldyrev, A. I. Revealing intuitively assessable chemical bonding patterns in organic aromatic molecules via adaptive natural density partitioning. *J. Org. Chem.* **73**, 9251–9258 (2008).
 39. Blanco, M. A., Martín Pendás, A. & Francisco, E. Interacting quantum atoms: a correlated energy decomposition scheme based on the quantum theory of atoms in molecules. *J. Chem. Theory Comput.* **1**, 1096–1109 (2005).
 40. Pyykkö, P. Additive covalent radii for single-, double-, and triple-bonded molecules and tetrahedrally bonded crystals: a summary. *J. Phys. Chem. A* **119**, 2326–2337 (2015).
 41. Alvarez, S. A cartography of the van der Waals territories. *Dalt. Trans.* **42**, 8617–8636 (2013).
 42. Foroutan-Nejad, C. The Na··· B Bond in NaBH₃[−]: A Different Type of Bond. *Angew. Chemie* **132**, 21086–21089 (2020).